Kang et al. Journal of Analytical Science and Technology 2013, 4:20
http://www.jast-journal.com/content/4/1/20

Journal of Analytical Science and Technology
a SpringerOpen Journal

RESEARCH Open Access

Optical characteristics and photothermal conversion of natural iron oxide colloid

Tae Yeon Kang[1], Ki Soo Chang[2], Jae Young Kim[2], Seon-Kang Choi[3] and Weon-Sik Chae[1*]

Abstract

Background: Chemical compositions and spectroscopic characteristics of the natural floating colloids in brine mineral water were investigated in this study.

Methods: The natural colloidal materials were investigated using electron microscopy, X-ray crystallography, elemental analysis, and absorption and emission spectroscopies.

Results: The natural colloidal particles have a spherical shape, with average diameter of 200 nm, and amorphous crystalline structure. The colloids are mostly composed of iron and oxygen atoms; they also contained small amounts of trace elements and rare earth minerals. In particular, the colloids show remarkable absorption and emission characteristics in the wide spectral region from ultraviolet (UV) to near infrared (NIR), which could make it useful in photoconversion and hyperthermal applications.

Conclusion: From the photothermal conversion efficiency measurement using an infrared thermography under irradiation of visible and NIR light, interestingly, it was found that the natural colloids have higher photothermal conversion efficiency, as compared with those of several different-typed minerals.

Keywords: Natural colloid; Geumjin spring water; Rare earth mineral; Near-infrared emission; Photothermal conversion

Background

Brine mineral water (BMW) is defined as any spring water that is gushed out from the bedrock located within about 1 km from the coast generally. BMW is known to include more abundant mineral ingredients, such as calcium (Ca), magnesium (Mg), strontium (Sr), manganese (Mn), zinc (Zn), nickel (Ni), and iron (Fe) in comparison with other ocean deep water. Moreover, BMW has an excellent mineral balance similar to that of human body fluids (Kim et al. 2008; Moon et al. 2004). Recently, BMW drawn from 1,100 m below the coast terrace of Geumjin (GJ) area (Gangneung City, Republic of Korea) has attracted special attention because it contains several functional minerals such as selenium (Se) and vanadium (V). Moreover, it is confirmed that this BMW has the most suitable mineral balance for Ca and Mg particularly because it is helpful for absorbing Ca to the human body. Using this unique BMW from the GJ area (GJ BMW), many studies have been recently performed in the various fields of industry, like functional food, cosmetics, and medicine. Kim et al. (2010) reported for the effect of the GJ BMW on atopic dermatitis *in vivo* with atopic dermatitis model. They have shown that the GJ BMW can not only suppress the ear swelling induced by trimellitic anhydride (TMA) but also attenuate hyperactivated lymph nodes stimulated by TMA. Moreover, they reported that the growth of several kinds of cancer cells was inhibited by GJ BMW through a dose-dependent manner (Kim et al. 2009). Contrary to the various studies and the practical uses of the GJ BMW, however, the floating colloidal particles, which are observed in the GJ BMW, are still not well known. These colloidal particles are suspended in high concentration in the GJ BMW, and they cause the GJ BMW to have a unique opaque color like red wine. However, after several hours, the floating colloids are mostly deposited on the bottom by self-aggregation. By now, there has been no systematic study on these sediments. In this work, we report on the

* Correspondence: wschae@kbsi.re.kr
[1]Gangneung Center, Korea Basic Science Institute (KBSI), Gangneung 210-702, Republic of Korea
Full list of author information is available at the end of the article

chemical compositions and spectroscopic properties of the natural colloidal particles in the GJ BMW. The optical properties of the colloidal particles were investigated by ultraviolet–visible (UV–vis) absorption and near-infrared photoluminescence (NIR-PL) spectroscopies and then their photothermal conversion characteristics were compared with those of the other mineral materials by infrared (IR) thermography. Here, we first report the unique optical characteristics of broad vis-NIR absorption and intense NIR emissions from the natural colloidal material. Interestingly, the colloidal material shows notable photothermal conversion property.

Methods

Sampling

BMW were collected at the Geumjin spring area located in the Gangneung City in the east region of the Republic of Korea (Figure 1). The BMW is originally a clear solution, but its color gradually turns to red orange with time under ambient condition. The red orange colloidal particles were typically sedimented within a day. The sedimented colloidal particles in the spring water were collected by centrifugation and then rinsed thoroughly with deionized (DI) water. The samples were dried at 100°C for 24 h in an oven, which were further used for all analyses and measurements.

Morphology and composition characterization

To study the particle formation kinetics, dynamic light scattering (DLS) measurement values were examined using an electrophoretic light scattering spectrophotometer (ELS-8000, Otsuka Electronics Co., Ltd., Osaka, Japan). The shape and size of the GJ colloidal particles were analyzed using a field emission scanning electron microscope (FESEM, SU-70, Hitachi Ltd. Tokyo, Japan) operating at 15-kV accelerating voltage. Powder X-ray diffraction crystallography (XRD) patterns were obtained with an X-ray diffractometer (X'Pert Pro, PANalytical, Almelo, The Netherlands). Elemental composition was determined using an energy dispersive X-ray spectrometer (EDS) which is attached to the FESEM. More quantitative analysis of trace elements in the GJ colloidal particles was performed by inductive coupled plasma mass spectrophotometry (ICP-MS) (Elan DRCII, Perkin

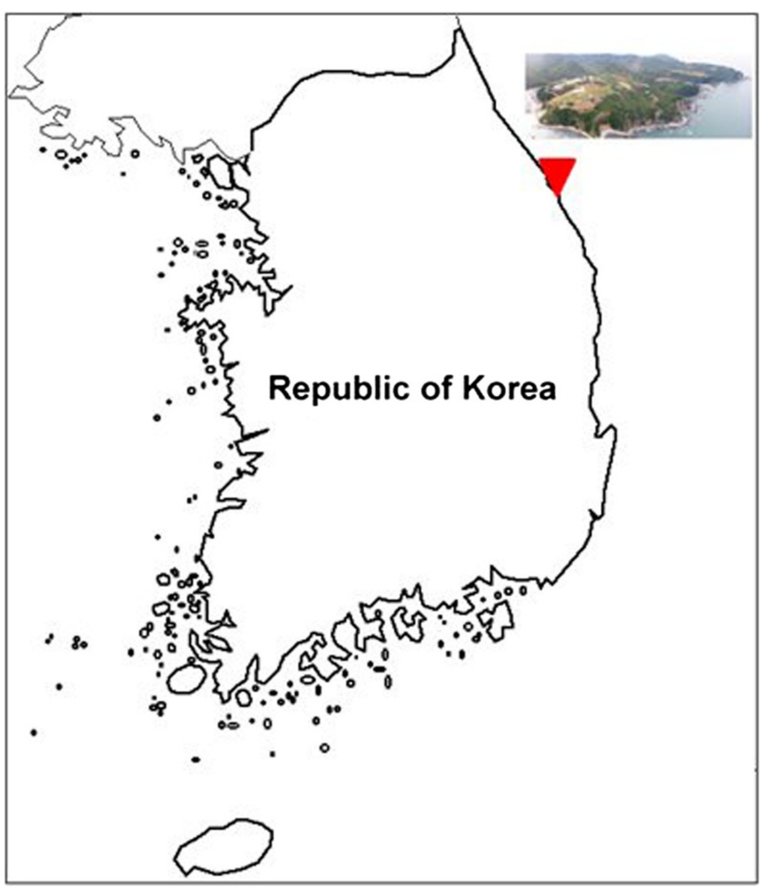

Figure 1 Geologic location of the Geumjin spring waters sampled in the Gangneung City, Republic of Korea.

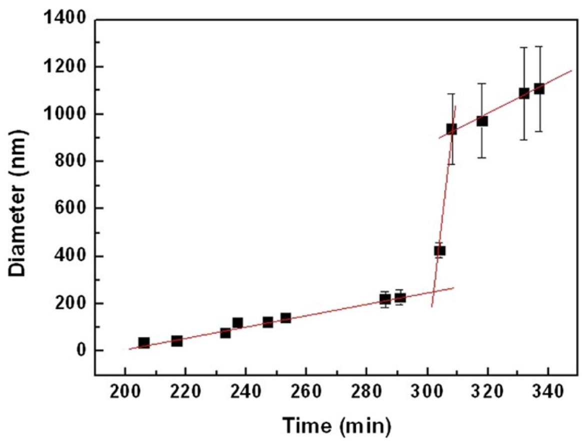

Figure 2 DLS measurement for colloidal particle size variation with time.

Elmer, Santa Clara, CA, USA) and inductively coupled plasma atomic emission spectrometry (ICP-AES) (JY Ultima2C, Jobin Yvon, Paris, France).

Spectroscopic characterization

UV–vis absorption spectrum of the GJ colloidal particles which are dispersed in ethylene glycol was recorded immediately using an UV–vis spectrophotometer (S-3100, Scinco Co., Ltd., Seoul, South Korea) at room temperature. A conventional quartz cuvette of 1-cm optical path was used for the measurements.

NIR photoluminescence (PL) spectrum of the GJ colloidal particles was also measured on a spectrophotometer (iHRA-330 PL, Jobin Yvon, Horiba) equipped with a liquid nitrogen-cooled InGaAs photodetector in a wavelength range of 800 to 1500 nm with a monochromatic 580-nm light (Xe lamp) as an excitation source.

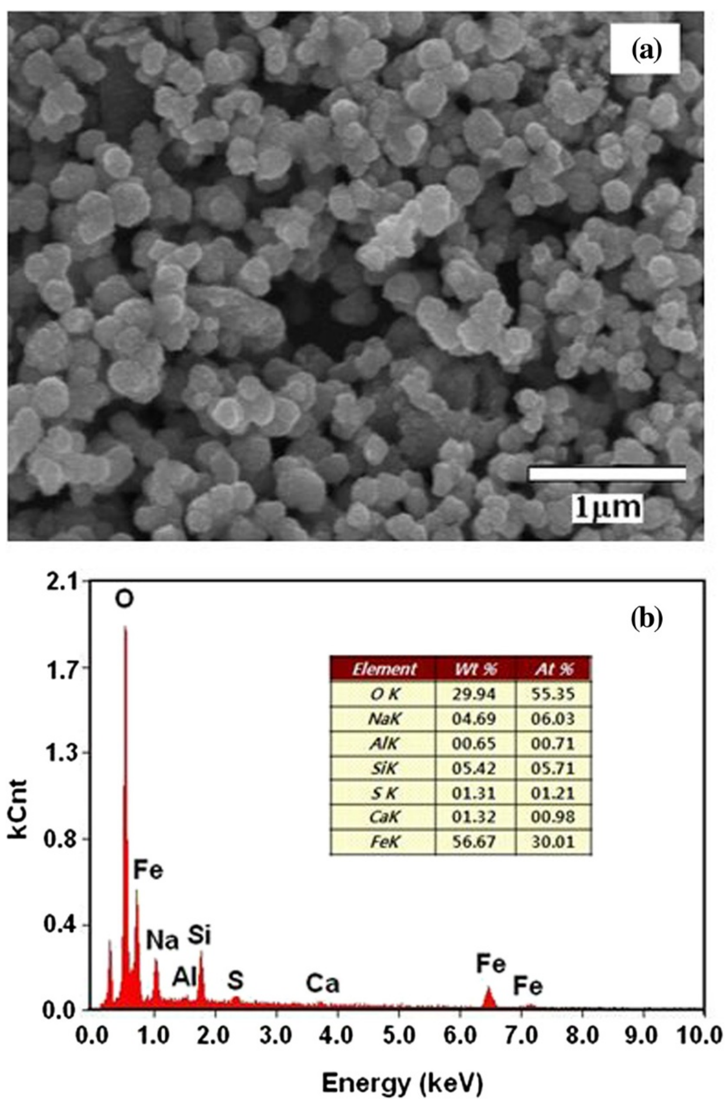

Figure 3 A SEM image (a) and an EDS spectrum (b) of the GJ colloidal particles.

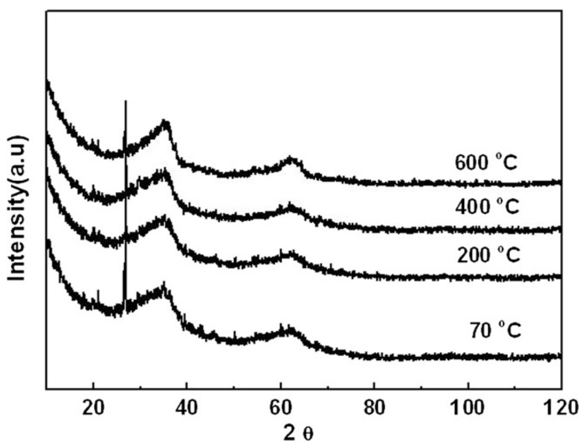

Figure 4 XRD patterns of the calcined colloidal powders treated at different temperatures in air for 5 h. We cannot assign the sharp peak at 27° at present.

Photothermal conversion measurements

Halogen illuminator (FHL-101, 100 W, Asahi-Spectra Co., Ltd., Tokyo, Japan) was used as a visible-NIR light source. The illuminating light from FHL-101 was delivered to the surface of the sample by fiber optic ring light guide (MRG53-1000S, Moritex Corp., Saitama, Japan). The distance between the sample surface and the fiber optic ring was about 8 cm. The illumination power was fixed at 200 mW/cm^2 at the sample surface. After light illumination, the temperature change of the samples was recorded using an infrared thermal camera (SC7600, FLIR Systems, Croissy-Beaubourg, France), every 10 s for 30 min. All the dispersed samples (10 mg/10 ml DI water) were placed in Teflon bath (10-mm diameter, 500 μl).

Results and discussion

Red orange colloidal particles were first formed in the GJ BMW, further grew, and sedimented with time. The sedimentation kinetics of the GJ colloidal particles were investigated by DLS measurements. Figure 2 shows the particle size variation for the GJ colloidal particles as a function of time. The red orange colloidal particles appeared after around 3 h and further increased in size as time goes on. After about 5 h, the size of the colloidal particles increased to around 200 nm and then the particles rapidly agglomerated to larger ones with an average size of 1 μm.

A FESEM image and an EDS spectrum of the GJ colloidal particles are shown in Figure 3. The colloidal particles have spherical shape and with about 200 nm in diameter; the primary colloidal particles aggregated by tens, which well agreed with the DLS results. The EDS analysis reveals that the colloidal particles are mainly composed of Fe and oxygen (O) with a minor number of minerals, such as sodium (Na), silicon (Si), and aluminum (Al).

The crystal structure of the colloidal particles was investigated by XRD analysis. The colloidal powder samples were calcined at 70°C, 200°C, 400°C, and 600°C in air for 5 h, respectively, which were further used for the XRD analysis. As shown in Figure 4, the

Table 1 Analysis of the GJ colloid powder by ICP-AES

Element	Concentration (ppm)
Al	14,050
Ca	32,090
Fe	411,100
K	2,873
Mg	3,263
P	115.3
Ti	468.9
Mn	86.38
Na	873.7
Pb	133.0

Resolution: 0.005 nm (UV) and 0.05 nm (visible). 0.07 g of the powder sample was used.

Table 2 Analysis of the GJ colloid powder by ICP-MS

Element	Concentration (ppb)
Ti	551,829
V	2,384
Cr	148,264
Ni	9,030
Cu	902,819
Zn	33,141
As	49,894
Rb	17,418
Sr	728,497
Y	5,453
Zr	13,756
Ag	801
Ba	107,025
Ce	7,452
Pr	815
Nd	4,355
Sm	716
Gd	1,107
Dy	616
Er	380
Yb	291
Pb	156,200
Th	1,724
U	470

Resolution: 0.005 nm (UV) and 0.05 nm (visible). 0.07 g of the powder sample was used.

measured XRD patterns do not show any distinct diffraction peak except two broad diffractions at approximately 35° and 62° for all colloidal samples. This means that the GJ colloidal particles have amorphous structural characteristics in crystallography, and this unique structural feature does not be much changed even for the heat-treated colloids at high temperature. A very similar XRD pattern was previously observed for the amorphous iron oxide/hydroxide materials (Kwon et al. 2005). In the case of the GJ colloid, the amorphous structure may be additionally attributed to the number of co-doped chemical compositions to the iron oxide matrix, as described below.

The chemical compositions of the GJ colloidal powder were determined by ICP-AES and ICP-MS (Tables 1 and 2). It shows very high concentrations of Fe (approximately above 40%) and some trace elements, such as Ca, Al, Mg, and K. Moreover, the GJ colloid also contains quite some amount of functional minerals (Se and V) as well as various rare earth minerals (Y, Ce, Nd, etc.). These functional minerals and rare earth minerals would be extremely useful in a variety of applied fields.

Absorption and photoluminescence spectrum of the GJ colloid, which is dispersed in ethylene glycol, are shown in Figure 5. The absorption spectrum (Figure 5a) shows broad absorption features from 350 to 900 nm with a maximum peak at 580 nm. This wide-range absorption means that the GJ colloidal particles can be utilized as a photoabsorber for the visible and infrared light. Figure 5b shows the photoluminescence spectrum of the GJ colloid at room temperature under the excitation wavelength of 580 nm. Interestingly, intense characteristic emissions are observed at the near-infrared regions (800 to 1,400 nm). Recently, NIR irradiation combined with NIR absorbing agents play a crucial role in the biomedical applications of anticancer treatment, hyperthermia therapy, and *in vivo* molecular imaging (Park et al. 2009; Lee et al. 2010; Park et al. 2010; Park et al. 2008). This is because the NIR light can penetrate deeply into the skin tissue and then this enables local heating to destroy target cancer cells by the assistance of NIR absorber and heating complex agents. This method enables an efficient anticancer treatment route without undesired side effects to normal organs and tissues (Sherlock et al. 2011). Moreover, NIR fluorophores offer better advantages than visible light fluorophores in molecular imaging applications. By now, quantum dots and rare earth metal reagents have been widely developed and studied in order to be used as NIR emitting probes (Ogawa et al. 2009; Sharma et al. 2008; Weissleder 2001). However, for the first time, at the best of our knowledge, we observed the presence of intense NIR emission from the natural colloidal product of iron oxide as main constituents. In the case of the GJ colloid, although it contains various co-doped elements, these broad and intense PL emissions may be attributed to the electronic transitions between the partly filled *d* electronic states (*d-d* transitions) of iron coupled with oxygen (Ronda 2007). In particular, the observed NIR emissions are well overlapped with the vibrational absorption (overtone and combination) bands of water molecule (Carleer et al. 1999). As a result, the NIR light absorbed by water can be efficiently transferred to heat by photothermal conversion process.

Hence, the extremely broad absorption and intense emission characteristics of the GJ colloids in the vis-NIR range could make it possible to cause a photothermal conversion with high efficiency. The photothermal conversion ability of the GJ colloid was measured by monitoring the temperature change during light irradiation. Figure 6 shows the temperature enhancement of the GJ colloid powder/water mixture (10 mg/10 ml), compared to pure DI water as a reference. The overall illumination power was approximately 200 mW/cm^2. The temperature of the GJ colloid powder/water mixture (0.5 ml) and pure water (0.5 ml) was increased to 30.3°C and 29.1°C, respectively, as shown in Figure 6a. From the repetitive

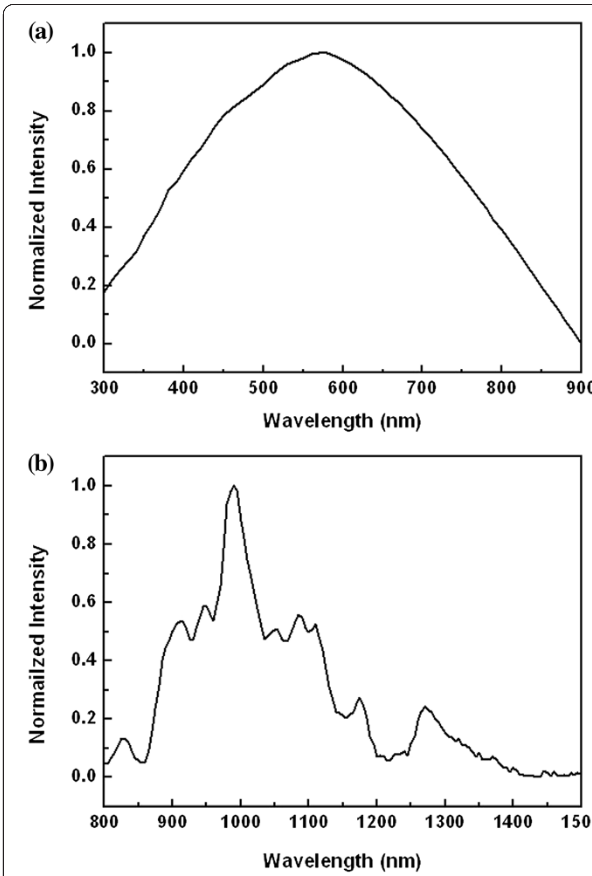

Figure 5 Absorption (a) and NIR emission (b) spectra of the GJ colloidal material dispersed in ethylene glycol. The excitation wavelength is 580 nm.

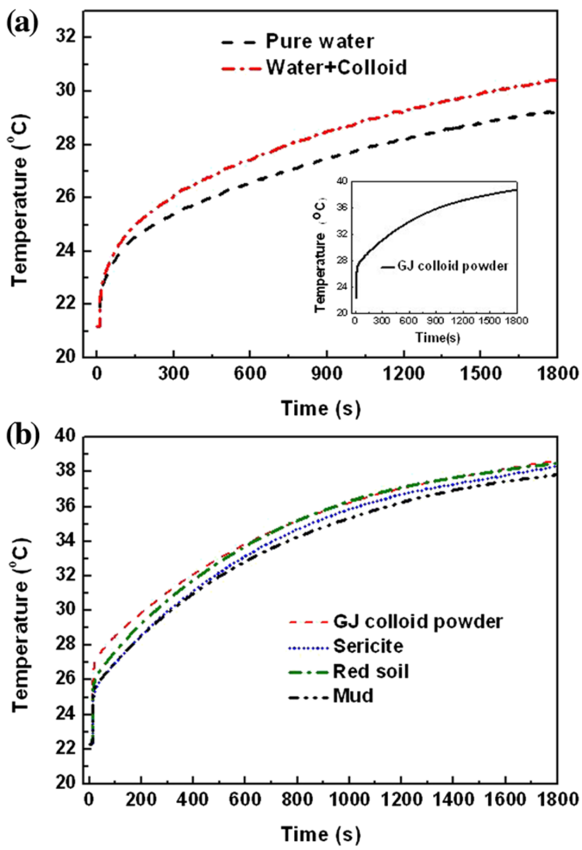

Figure 6 Temperature changes. (a) Temperature change of the GJ colloidal powder/water mixture (10 mg/10 ml) and pure DI water under visible and NIR light irradiation for 30 min. Inset: temperature change of the GJ colloid powder itself under the same light irradiation and detection conditions. **(b)** Temperature change of the GJ colloid powder, red soil, sericite, and mud under visible and NIR irradiation for 30 min.

measurements, it is consistently observed that the temperature of the GJ colloid powder/water mixture was more enhanced than that of pure DI water under the same conditions. This enhanced temperature elevation can be assigned to the direct energy transfer of the emissions of the GJ colloid by the vibrational absorptions of water, as mentioned above. In addition, light energy absorbed by the GJ colloidal powder itself can be also converted to heat and then be transferred to water. The inset in Figure 6a depicts the temperature change of the GJ colloidal powder itself under visible and NIR irradiation for 30 min. The temperature of the GJ colloidal powder was drastically increased up to approximately 38.5°C. This indicates that the absorbed light energy in the excited states of iron oxide moiety can be transferred to thermal energy through nonradiative intramolecular vibrational relaxations and/or transitions (Jackson et al. 1981). Hence, photothermal conversion efficiency measurements were also performed for similar natural materials, such as red soil, sericite, and mud. Under the same conditions, the GJ colloidal powder showed the best photothermal conversion efficiency for all measurement time, as compared to those of the other similar natural materials (Figure 6b). Approximating similar self-heating effects of the natural materials themselves through nonradiative vibrational relaxations, it is considered that this superior photothermal conversion ability of the GJ colloid is due to the wide absorption characteristics for visible-NIR light and subsequent efficient energy transfer processes of the excited electronic energy of the colloid to excite vibrational modes of surrounding water.

Conclusion

We have investigated for the composition, structure, and optical characteristics, and photothermal conversion efficiency of the floating colloidal particles in brine mineral water at the Geumjin area. In this study, we first observed unique optical characteristics of broad vis-NIR absorption and intense NIR emissions from the natural colloidal material including additional co-doped elements. The colloidal material shows notable photothermal conversion efficiency compared to the other natural products. The obtained results show that the GJ colloidal particles would have distinctive promise for use in various fields, such as therapeutic and biomedical diagnosis applications in addition to conventional photothermal therapy.

Competing interests

The authors declare that they have no competing interests.

Authors' contributions

WSC designed the study. TYK and WSC performed the research. KSC and JYK carried out the photothermal analysis. SKC did the sampling of the materials. TYK and WSC wrote the manuscript. All authors read and approved the final manuscript.

Acknowledgements

This work was supported by a grant (no. PGB066) from the Catholic University of Korea (Seoul St. Mary's Hospital), a grant (no. K3208F) from the Korea Basic Science Institute (KBSI), and partly by a KRF grant (no. 2011–0008671). We thank the Korea Basic Science Institute, Seoul Center (Seoul, Korea) for the help with the ICP-AES and ICP-MS measurements.

Author details

[1]Gangneung Center, Korea Basic Science Institute (KBSI), Gangneung 210-702, Republic of Korea. [2]Center for Analytical Instrumentation Development, Korea Basic Science Institute (KBSI), Daejeon 305-806, Republic of Korea. [3]Tongyang Life Science Corp., Seoul 135-995, Republic of Korea.

Received: 4 September 2013 Accepted: 17 October 2013
Published: 15 Nov 2013

References

Carleer M, Jenouvrier A, Vandaele AC, Bernath PF, Me´rienne MF, Colin R, Zobov NF, Polyansky OL, Tennyson J, Savin VA (1999) The near infrared, visible, and near ultraviolet overtone spectrum of water. J Chem Phys 111:2444–2450

Jackson WB, Amer NM, Boccara AC, Fournier D (1981) Photothermal deflection spectroscopy and detection. Appl Optics 20:1333–1344

Kim YJ, Jung IS, Song HJ, Choi EY, Choi IS, Choi YJ (2008) Study of deep ground sea-like water on antioxidant activity and the immune response in RAW264.7 macrophages. J Life Sci 18:329–335

Kim WJ, Li H, Yoon TJ, Sim JM, Choi SK, Lee KH (2009) Inhibitory activity of brine mineral water on counter cell growth, materials and angiogenesis. Korean J Food Nut 22:542–547

Kim JJ, Kim WJ, Sim JM, Choi SK, Kwon SS, Kim JD, Lee KH (2010) Effect of brine mineral water on TMA-induced contact hypersensitivity reaction in the mouse model. Korean J Food Nut 23:440–445

Kwon SK, Kimijima K, Kanie K, Muramatsu A, Suzuki S, Matsubara E, Waseda Y (2005) Inhibition of conversion process from $Fe(OH)_3$ to β-FeOOH and α-Fe_2O_3 by the addition of silicate ions. ISIJ Int 45:77–81

Lee SM, Park H, Yoo KH (2010) Synergistic cancer therapeutic effects of locally delivered drug and heat using multifunctional nanoparticles. Adv Mater 22:4049–4053

Moon DS, Jung HJ, Kim HJ, Shin PK (2004) Comparative analysis on resources characteristics of deep ocean water and brine groundwater. J Kor Soc Mar Environ Engi 7:42–46

Ogawa M, Kosaka N, Choyke PL, Kobayashi H (2009) In vivo molecular imaging of cancer with a quenching near-infrared fluorescent probe using conjugates of monoclonal antibodies and indocyanine green. Cancer Res 69:1268–1272

Park H, Yang J, Seo S, Kim K, Suh J, Kim D, Haam S, Yoo KH (2008) Multifunctional nanoparticles for photothermally controlled drug delivery and magnetic resonance imaging enhancement. Small 4:192–196

Park H, Yang J, Lee J, Haam S, Choi IH, Yoo KH (2009) Multifunctional nanoparticles for combined doxorubicin and photothermal treatments. ACS Nano 3:2919–2926

Park JH, Von Maltzahn G, Xu MJ, Fogal V, Kotamraju VR, Ruoslahti E, Bhatia SN, Sailor MJ (2010) Cooperative nanomaterial system to sensitize, target, and treat tumors. Proc Natl Acad Sci USA 107:981–986

Ronda C (2007) Luminescence: from theory to applications. Wiley, New York

Sharma R, Wendt JA, Rasmussen JC, Adams KE, Marshall MV, Sevick-Muraca EM (2008) New horizons for imaging lymphatic function. Ann N Y Acad Sci 1131:13–36

Sherlock SP, Tabakman SM, Xie L, Dai H (2011) Photothermally enhanced drug delivery by ultrasmall multifunctional FeCo/graphitic shell nanocrystals. ACS Nano 5:1505–1512

Weissleder R (2001) A clearer vision for in vivo imaging. Nat Biotechnol 19:316–317

10.1186/2093-3371-4-20
Cite this article as: Kang *et al.*: Optical characteristics and photothermal conversion of natural iron oxide colloid. *Journal of Analytical Science and Technology* 2013, 4:20